Photonic Vitrimer Elastomer with Self-Healing, High Toughness, Mechanochromism, and Excellent Durability based on Dynamic Covalent Bond

Wenbin Niu, Xianfei Cao, Yunpeng Wang, Bowen Yao, Yusen Zhao, Jie Cheng, Suli Wu, Shufen Zhang, and Ximin He**

Vitrimers, with their unique dynamic covalent bonds, possess attractive self-healability and mechanical robustness, providing an intriguing opportunity to construct functional soft materials. However, their potential for function recovery, especially optical function, is underexplored. Harnessing the synergistic effect of photonic crystals and vitrimers, a novel photonic vitrimer with light regulating and self-healing capabilities is presented. The resulting photonic vitrimer exhibits a large tensile strain (>1000%), high toughness (21.2 kJ m^{-3}), bright structural color, and mechanochromism. Notably, the structural color remains constant even after 10 000 stretching/releasing cycles, showing superior mechanical stability, creep-resistance, and excellent durability. More importantly, the exchange of dynamic covalent bonds imparts the photonic vitrimer with a self-healing ability (>95% efficiency), enabling the recovery of its optical function. Benefiting from the above merits, the photonic vitrimer has been successfully used as a sensor for human motion detection, which demonstrates visualized interactive sensibility even after self-repairing. This material design provides a general strategy for optical functionalization of vitrimers. The photonic vitrimer elastomers present great potential as resilient functional soft materials for diverse flexible devices and a novel optical platform for soft robotics, smart wearable devices, and human-machine interaction.

1. Introduction

As technology advances, people raise new requirements for lightweight functional polymeric materials, owing to their accelerated applications in a variety of emerging fields such as smart wearable devices,[1] energy,[2] display,[3] sensing,[4] and healthcare.[5] For example, current wearable sensors that monitor bodily motions and functions under repetitive stretching and bending inevitably suffer from structural or mechanical damage and thus functional failure. These emerging flexible or wearable devices demand the functional polymeric materials to have not only high mechanical robustness but also the ability to recover their functions during practical applications even when subject to damage. Conventional polymer materials are difficult to satisfy the above demands due to their limited repairing capability and poor reconfigurability.[6] Self-healable polymeric materials are capable of repairing internal and external damages, thereby enhancing material reliability and prolonging service life. To date, several strategies have been proposed to achieve the self-healing of polymer networks through intra/inter-molecular interactions, including hydrogen bonds,[7] ion coordination bonds,[8] dynamic covalent bonds,[9] and so on. Characterized by dynamic covalent bonds, vitrimers are able to reconfigure their network topology to achieve self-healing through bond exchange reactions under external stimuli, such as thermal or light.[10] Compared with other self-healing systems, the elastomers based on dynamic covalent bonds show high mechanical properties (such as strength, toughness),[8b] good creep- and chemical-resistance, and high dimensional stability.[9] Currently, great advances have been made in improving the shape and mechanical-recovery performances of vitrimers.[9,10] However, since the functional vitrimers are usually a composition of vitrimers and functional substances, it remains a great challenge to achieve functional recovery even though the vitrimer itself could be repaired. Although there have been a few reports on self-healing electrical vitrimers,[2,11] the self-repairing of optical functional vitrimers is rarely reported.

As a remarkable class of advanced optical materials, photonic crystals could regulate the traveling of light through periodic nanostructures with different dielectrics,[12] giving rise to

Prof. W. Niu, X. Cao, Y. Wang, J. Cheng, Prof. S. Wu, Prof. S. Zhang
State Key Laboratory of Fine Chemicals
Dalian University of Technology
West Campus, 2 Linggong Rd., Dalian 116024, China
E-mail: niuwb@dlut.edu.cn
B. Yao, Y. Zhao, Prof. X. He
Department of Materials Science and Engineering
University of California
Los Angeles, CA 90095, USA
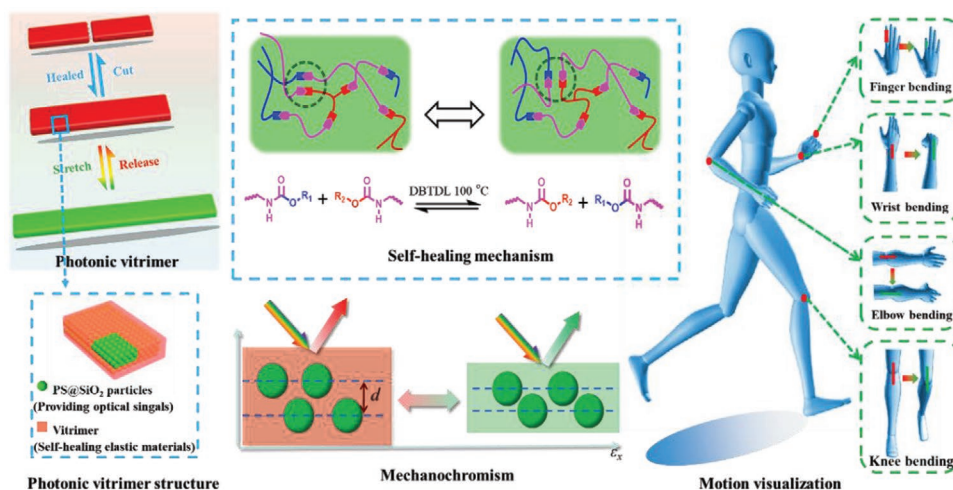E-mail: ximinhe@ucla.edu

2009017 (1 of 9)

Figure 1. Schematics of the structure, the dynamic covalent cross-linking network, the mechanochromic mechanism, and the motion-sensing of the photonic vitrimer.

brilliant structural colors like the dazzling examples in nature (e.g., butterflies,[13] chameleons,[14] and so on).[15,16] Integrating self-healing polymeric networks with photonic crystals could create photonic crystals with self-healing capability, leading to potential applications in visualized human-machine interface,[17] smart wearable interactive sensor,[3a] and cell monitoring.[18] However, the existing self-healable photonic crystals are based on hydrogels or supramolecular elastomers with weak hydrogen/coordination bonding,[17e,f] which usually suffers from low ambient stability, weak mechanical properties, and poor creep-resistance. The introduction of vitrimer polymer networks with relatively strong covalent bonds would render the self-healable photonic crystals with high ambient stability, excellent mechanical properties, creep-resistance, and durability. Meanwhile, the photonic crystal structure would provide the vitrimers with healable optical function. However, the combination of the photonic crystals and vitrimers remains unexplored.

Herein, we present the first self-healable photonic vitrimer by integrating the photonic crystals with a new vitrimer elastomer (**Figure 1**). First, a series of new vitrimer elastomers were synthesized by polycondensation of hydroxyl-terminated polybutadiene (HTPB), polytetrahydrofuran (PTMG), glycerol (GLY), and isocyanate (IPDI) molecules. By introducing photonic crystals, the resultant photonic vitrimer not only retains the properties of the vitrimer itself, but also is imparted with appealing optical functions, specifically bright structural color and color-changing ability under strain (i.e., mechanochromism). Therefore, compared with photonic hydrogels and supramolecular photonic elastomers, the photonic vitrimer exhibits high toughness, large strength, excellent optical creep-resistance, and excellent durability. Importantly, by exploiting the synergy of photonic crystal bandgap and dynamic covalent network, it is demonstrated that the photonic vitrimer had self-repairing capability of structural color and visualized mechanochromism during stretching. The resultant photonic vitrimer could be used as an interactive sensor for visual monitoring human motion without an external power supply, even when the sensor is repaired after damage, showing great promise in self-reporting smart wearable devices, health monitoring, and human-machine interaction.

2. Results and Discussion

2.1. Synthesis and Characterization of Vitrimer Elastomer

In a typical experiment, covalent cross-linked vitrimer elastomers were prepared through polycondensation of HTPB, PTMG, GLY, and IPDI in the presence of dibutyltin dilaurate (DBTDL) catalysis, as shown in **Figure 2**a. It can be seen from Fourier transform infrared (FT-IR) spectra that HTPB, PTMG, and GLY show broad absorption bands at ≈ 3300 to 3500 cm^{-1} ascribed to stretching vibrations of -OH groups; IPDI displays characteristic peak of $-N=C=O$ group at 2300 cm^{-1}. Those characteristic peaks vanish after reaction, while the absorption peak at 1700 cm^{-1} is attributed to carbamate C=O group appears, indicating the formation of a covalent cross-linking vitrimer network (Figure 1b). The appearance of the proton chemical shift of carbamate bond at 8.7 ppm further verifies the above result (Figure S1, Supporting Information). In addition, X-ray photoelectron spectrum (XPS) profile shows the peaks of carbon and nitrogen elements at 289.1 and 399.8 eV binding energy, attributed to $-O-C=O$ and $C-N$ groups,[19] respectively, further implying the formation of carbamate C=O bond.

A series of vitrimer elastomers (Vitrimer-I to Vitrimer-XI) with distinct mechanical properties were obtained by regulating the amounts of HTPB, PTMG, and GLY (Table S1, Supporting Information). It is observed from the stress-strain curves that the vitrimer elastomers display fracture strains more than 1000%, and the stress and strain increase gradually with the increasing butanediol unit in the network (Figure S2, Supporting Information). This is due to the formation of hydrogen bonding between the butanediol segment and carbamate group and the relatively high ductility.[20] By contrast, the strength enhances while the elongation at break reduces
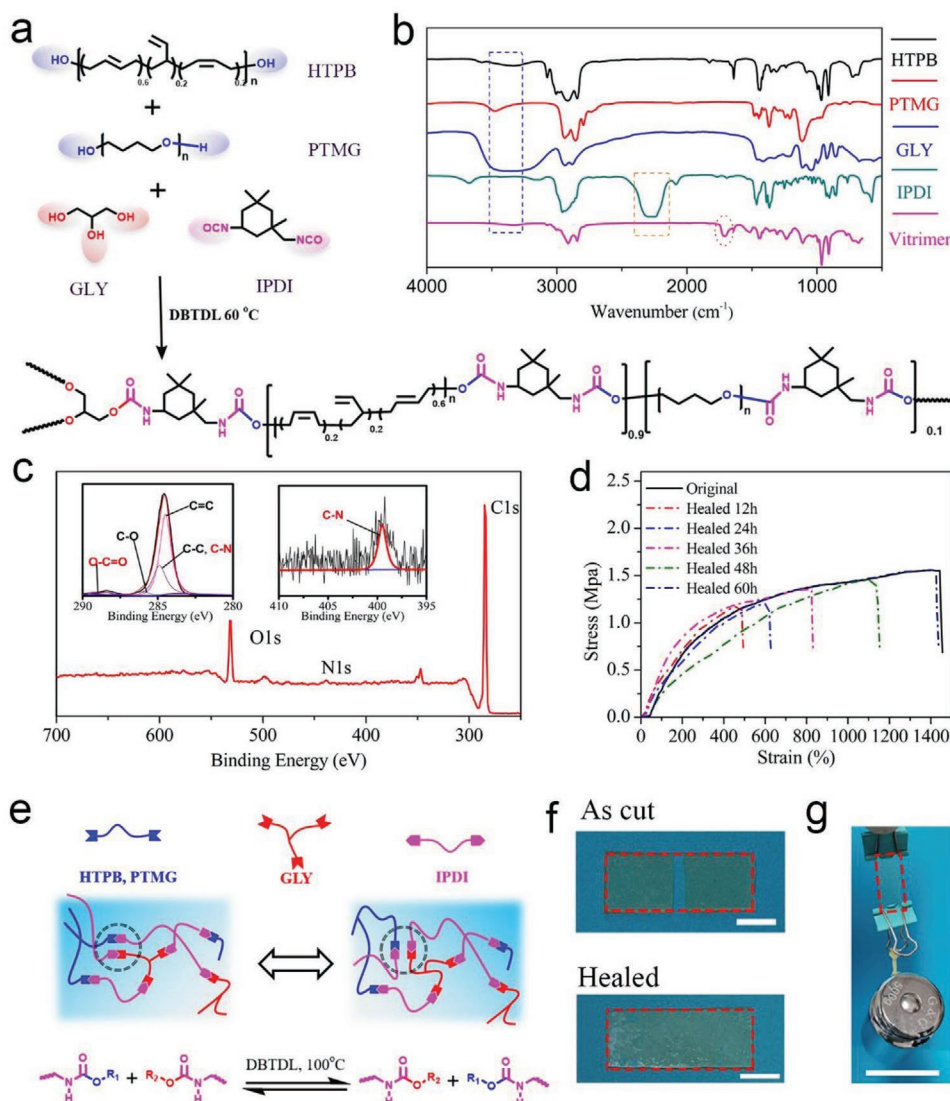
Figure 2. Preparation and characterization of vitrimer elastomers. a) Chemical structures of vitrimer elastomers. b) FT-IR spectra of precursors and vitrimer elastomers. c) XPS profile of vitrimer elastomer. d) Stress-strain curves of vitrimer–II before and after healing. e) Schematic illustration showing the self-healing mechanism of vitrimer elastomer. Photographs showing the typical self-healing behavior of vitrimer elastomer: f) as-cut crack and healed (100 °C for 60 h) sample (Scale bar: 1cm), and g) loading photo of the healed sample with a 500 g weight (Scale bar: 2.5cm).

(Figure S3, Supporting Information) with increasing GLY content, because the introduction of GLY crosslinker increases the network rigidity, resulting in a decrease in the elongation at break.

The dynamic carbamate bond endows the vitrimer elastomers with self-healing ability. To evaluate the self-healing ability, we measured and calculated the mechanical self-healing efficiency (Equation S1, Supporting Information) using Vitrimer-II sample as an example. Figure 2d displays the stress-strain curves of samples before and after self-healing at 100 °C for various healing durations. Apparently, the self-healing efficiency improves as the time prolongs, and the highest efficiency of 98% was obtained. Figure 2e illustrates a proposed self-healing mechanism based on the dynamic carbamate bond in a vitrimer elastomer.[11] The topological structure of the vitrimer

network is reconfigured with the exchange reaction of dynamic carbamate bond, granting the material with self-healing ability. With the prolongation of contact time, the probability to reform carbamate bond is increased, resulting in higher recovery efficiency. Scanning electron microscope (SEM) images (Figure S4, Supporting Information) and photographs intuitively reveal the repair of cracks and the recovery of mechanical properties, respectively, demonstrating excellent self-healing ability (Figure 2f,g). Although the self-healing temperature is a little bit high than some polyurethane materials reported previously,[21] most of them rely on weak coordination or hydrogen bonds cross-linking interactions, which usually suffer from low creep-resistance. In contrast, the strong chemical interaction endows the polyurethane materials with good creep-resistance and durability.

ADVANCED
SCIENCE NEWS
www.advancedsciencenews.com

ADVANCED
FUNCTIONAL
MATERIALS
www.afm-journal.de

2.2. Preparation and Optical Properties of Photonic Vitrimer

Taking advantage of the vitrimer elastomer, a photonic vitrimer composed of PS@SiO$_2$ opal photonic crystal embedded in vitrimer elastomer was prepared, as schematically displayed in **Figure 3**a, in which vitrimer-II with moderate strength and stretchability was used as elastic substrate. The resultant photonic vitrimer shows a bright structural color. It can be seen that the addition of vitrimer-II elastomer leads to the red-shift of reflection wavelength, which is determined by the Bragg diffraction law.[14,22] For example, the wavelength of opal photonic template shifts from 525 to 640 nm after infiltrating vitrimer elastomer. This is because the vitrimer elastomer replaces air in the photonic crystal template, which increases the effective refractive index. On the other hand, the infiltration of vitrimer elastomer increases lattice spacing, forming a non-closed packed structure, as demonstrated by cross-sectional SEM images in Figure 2d,e. As a result, the reflection wavelength exhibits red-shift according to the Bragg diffraction Equation S4, Supporting Information.

Importantly, the photonic vitrimer demonstrates good mechanochromism during the stretching process. The structural color undergoes a gradual shift from red to green as the sample is stretched from 0 to 85% strain, as displayed in Figure 2f. Accordingly, the reflection wavelength continuously moves from 640 to 540 nm (Figure 3g and Movie S1, Supporting Information). The continuous record of reflection spectra confirms the above color-changing process (Figure 3h).

During stretching, the thickness along observation direction (z) that is perpendicular to the tensile one (x) is reduced. The corresponding tensile strain (ε_z) can be expressed by the tensile strain in the x-direction (ε_x) and Poisson's ratio (v): $\varepsilon_z = -v\varepsilon_x$. Therefore, the reflection wavelength in stretched states can be modeled by the following Equation (1):

$$\lambda_{max} = 2d\left(1 - v\varepsilon_x\right)n_{eff} \tag{1}$$

$$n_{eff} = \left(n_{ps@sio2}^2\phi + n_{vitrimer}^2\left(1-\phi\right)\right)^{\frac{1}{2}} \tag{2}$$

where λ_{max}, d, n_{eff}, Φ, $n_{PS@SiO2}$, and $n_{vitrimer}$ represent the reflection wavelength, lattice spacing, effective refractive index of the photonic vitrimer, volume fraction of PS@SiO$_2$ microspheres, and refractive indices of PS@SiO$_2$ microspheres and vitrimer elastomer. A value of Φ 44% is calculated from Equations (1), (2), and Equations S3,S4, Supporting Information. According to Equation (1), the lattice spacing (d) along ε_z direction decreases with increasing tensile strain, and the wavelength shifts toward the short direction. This result is consistent with our experimental observation. In addition, there is a good linear relationship between wavelength and strain in a range of 0 to 40% (Figure S5, Supporting Information), suggesting that the deformation of photonic vitrimer is controlled by the elasticity of vitrimer itself. The wavelength change reduces with further increasing the tensile strain, owing to the proximity between microspheres.

Apart from optical function, the introduction of opal photonic crystal also enhances the toughness of vitrimer (16.9 kJ m^{-3}). In stress-strain curves, the maximum tensile stress is enhanced

while the elongation at break is slightly reduced after opal photonic crystal addition in comparison with that of pure vitrimer elastomer (Figure 3j). This is maybe due to the chemical interaction between vitrimer network and hydroxyl group on the surface of rigid PS@SiO$_2$ microsphere.[24] Therefore, the photonic vitrimer exhibits high toughness (21.2 kJ m^{-2}). Such toughness is much higher than those of photonic hydrogels and supramolecular photonic elastomers reported previously (Figure 3k), owing to relatively strong covalent bond in the vitrimer network.[2] Furthermore, the cross-linked covalent network avoids the sliding of molecular chains during stretching, thus the structural color and reflection wavelength almost remain constant during 10 000 continuous stretching-releasing cycles (Figure 3l and Figure S6, Supporting Information), demonstrating its excellent reversibility, creep-resistance, and durability. Such abilities enable the practical applications of the photonic elastomer as a powerful platform for interactive sensing.

2.3. Dynamic Mechanical Properties and Self-Healing of Photonic Vitrimer

To evaluate the dynamic properties of photonic vitrimer, we investigate glass transition temperature and temperature-dependent stress relaxation using a dynamic mechanical analyzer (DMA). It is shown that the glass transition temperature of vitrimer sample is about −57 °C (**Figure 4**a), which is consistent with that of the control vitrimer (Figure S7, Supporting Information), indicating its high elastic state at room temperature. Temperature-dependent stress relaxation experiments show that the relaxation time of normalized stress decreases gradually as temperature rises (Figure 4b), indicating that high temperature accelerates the movement of polymer chains and the exchange rate of carbamate bonds in the vitrimer dynamic networks. In a Maxwell viscoelastic fluid model, the relaxation time is defined as the time when the instantaneous stress changes to 1/e of its initial stress. According to Arrhenius's law: $\tau = \tau_0 \exp\left(\dfrac{E_a}{RT}\right)$, in which τ, T, τ_0, E_a, and R are, respectively, stress relaxation time, temperature, relaxation time at a determined temperature, stress relaxation activation energy, and gas constant. Evidently, the relaxation time decreases sharply with increasing temperature. The introduction of rigid PS@SiO$_2$ microspheres hinders the exchange of dynamic networks, reducing the exchange rate and thus prolonging the relaxation time (Figure 4b and Figure S8, Supporting Information). Correspondingly, the relaxation activation energy ($E_a = 83.55$ kJ mol^{-1}) of the photonic vitrimer transesterification reaction is also calculated (Figure 4c), which is larger than that of pure vitrimer (61.08 kJ mol^{-1}, Figure S9, Supporting Information). This result reveals that the photonic vitrimer is much sensitive to the temperature change than pure vitrimer. Therefore, the photonic vitrimer exhibits good stability at room temperature and a fast bond exchange rate at high temperature, enabling self-healing of shape, mechanical properties, and optical function.

Figure 4e exhibits stress-strain curves of the photonic vitrimer after healing at 100 °C for various times. The self-healing efficiency increases with healing duration, and a value of 95% is reached, which was calculated quantitatively via Equation S2,
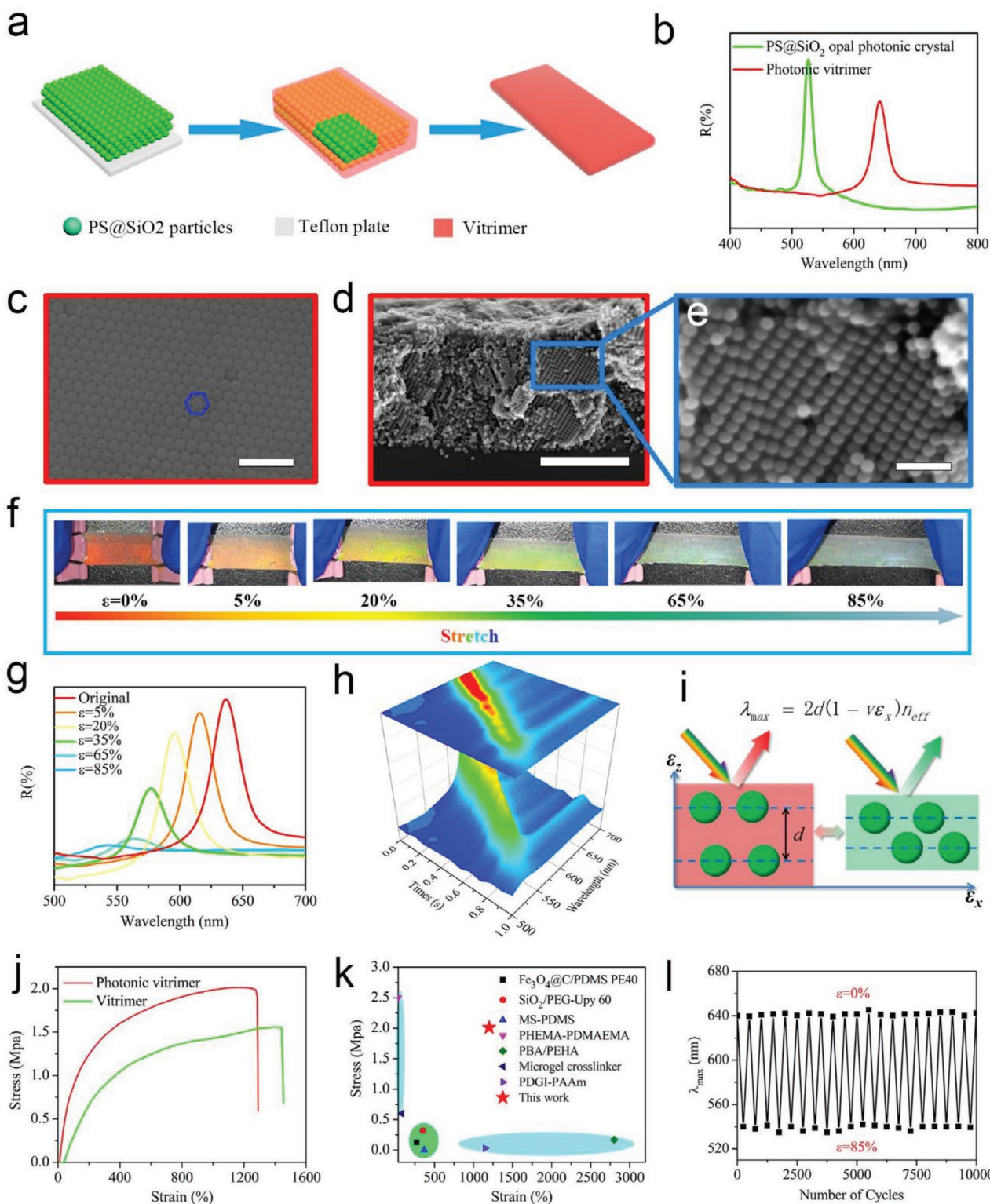
ADVANCED
SCIENCE NEWS
www.advancedsciencenews.com

ADVANCED
FUNCTIONAL
MATERIALS
www.afm-journal.de

Figure 3. Preparation and optical properties of photonic vitrimer. a) Schematic diagram showing the preparation of photonic vitrimer. b) Reflection spectra of PS@SiO$_2$ opal photonic crystal and photonic vitrimer. c) Top SEM image of PS@SiO$_2$ opal photonic crystal (Scale bar: 1 μm). Cross-sectional SEM images of the photonic vitrimer at d) low (Scale bar: 5 μm) and e) high (Scale bar:1 μm) magnification. f) Optical images (Sample: 2cmX1c-mX1mm) and g) reflection spectra of the photonic vitrimer under different tensile strains. h) 3D cartoon map showing reflection spectra of the photonic vitrimer during continuous stretching. i) Schematic illustration showing mechanochromic mechanism. j) Strain-stress curves of the vitrimer elastomer and photonic vitrimer. k) Comparison of the tensile strain and stress at fracture of our photonic vitrimer with those reported photonic hydrogels and supramolecular elastomers.[4b,17,23] l) Reflection wavelength changes of the photonic vitrimer during 10 000 stretching/releasing cycles at a strain of 85%.
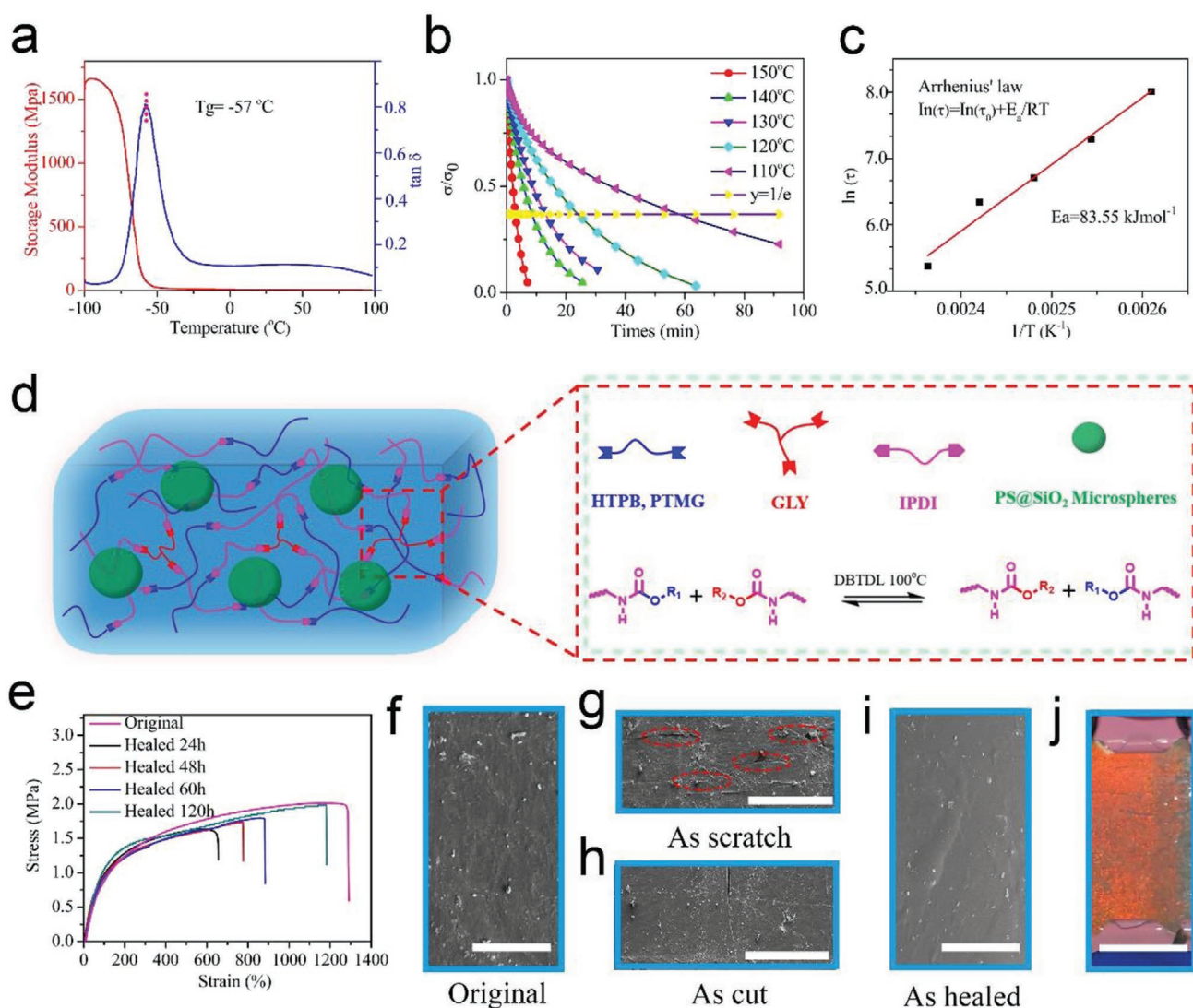
Figure 4. a) Temperature dependence of storage modulus and tan delta (δ) of the photonic vitrimer measured using dynamic mechanical analysis. b) A normalized stress relaxation curves of photonic vitrimer at different temperatures. c) Arrhenius analysis and photonic vitrimer network activation energy. d) Microstructure and dynamic network exchange mechanism diagram of the photonic vitrimer. e) Strain-stress curves of the photonic vitrimer after self-healing. SEM images of f) original, g) scratched (as indicated by red circles), h) cut, and i) self-healed photonic vitrimer surface (Scale bar: 500 µm). j) Optical image of the self-healed photonic vitrimer (Scale bar: 1 cm).

Supporting Information. Compared with the control sample, the self-healing time is significantly increased, indicating that the exchange rate of the carbamate bond decreases, which is consistent with the result of the DMA test. To directly demonstrate the self-healing ability, the photonic vitrimer surface was scratched and cut artificially. Figure 4f shows an SEM image of pristine photonic vitrimer surface. After scratching (Figure 4g) and cutting (Figure 4h) with a blade, the sample was then heat-treated (100 °C for 120 h). It is shown that these scratches and cut almost disappeared (Figure 4i), accompanying with flow trails of vitrimer elastomer. Moreover, the healed photonic vitrimer retains the bright structural color (Figure 4J), and the reflection peak position and intensity are consistent with the original one (Figure S10, Supporting Information). Particularly, the self-healed photonic vitrimer exhibits the same

mechanochromism behavior and wavelength-strain relationship during stretching (Figure S11, Supporting Information), confirming the repair of optical function.

2.4. Interactive Sensor Based on Photonic Vitrimer

Considering good mechanochromism, superior mechanical properties, and self-healing ability, the photonic vitrimer can be used as a visualized interactive sensor for tracking human motion. As illustrated in **Figure 5**a, human eyes can intuitively perceive the motion of joints via color changes when the sensor was attached to a finger, wrist, elbow, or knee. Figure 5b shows reflection spectra and photographs of the finger under stepwise bending, using a red photonic vitrimer as the interactive
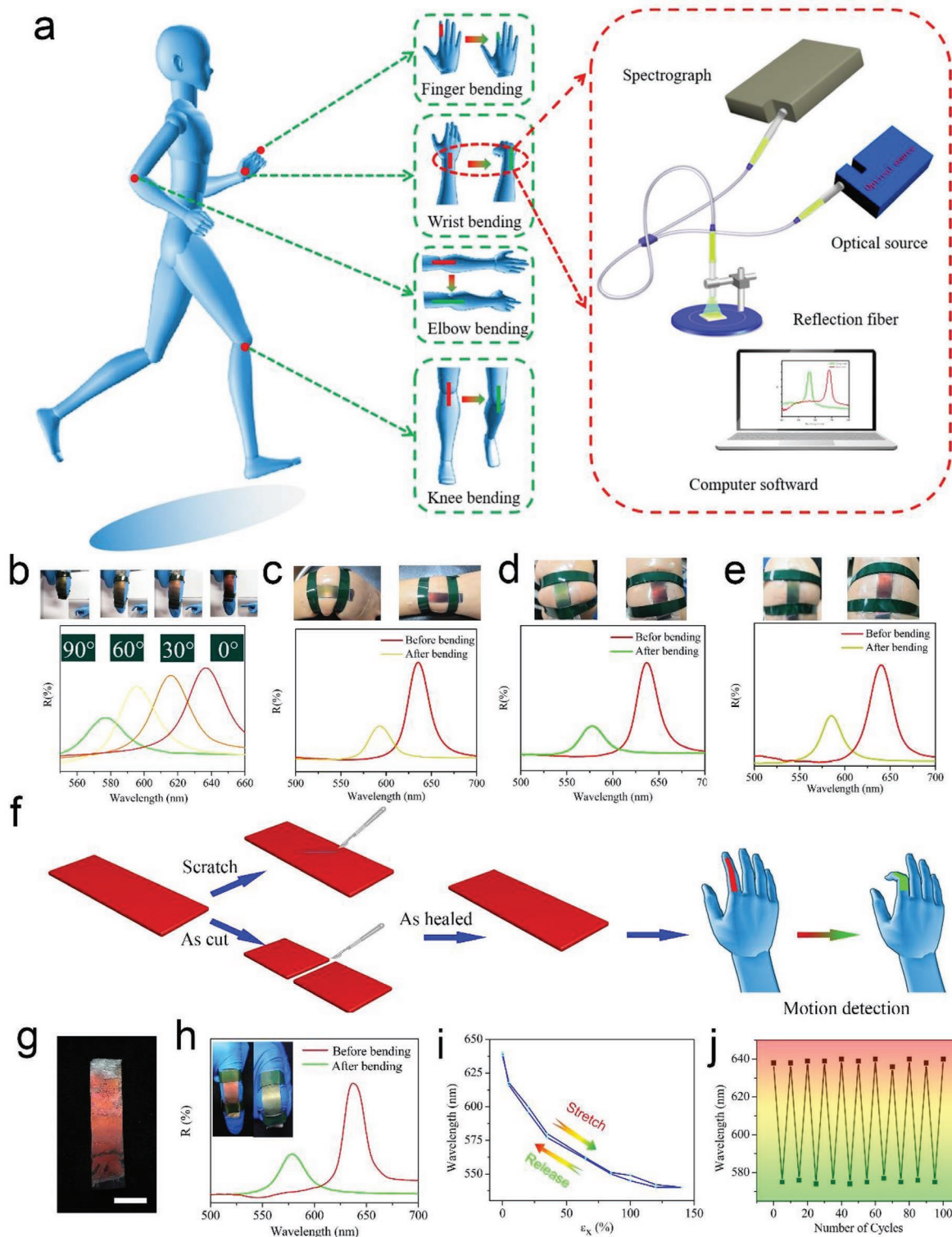
ADVANCED
SCIENCE NEWS
www.advancedsciencenews.com

ADVANCED
FUNCTIONAL
MATERIALS
www.afm-journal.de

Figure 5. a) Schematic illustration showing the application of photonic vitrimer as an interactive sensor for tracking human motion. b) Reflectance spectra of the interactive sensor used for finger motion-sensing under stepwise bending. The insets depict top- and side-view optical images during sensing. Reflectance spectra and optical images of the interactive sensor for detecting c) wrist, d) elbow, and e) knee joints movements. f) Schematic illustration showing the photonic vitrimer interactive sensor after self-repairing, when it suffers from scratch and fracture. g) Optical image of the self-healed sensor (Scale bar: 1cm). h) Reflectance spectra and digital photo images of the self-healed sensor for finger joint motion detection. i) The reflection wavelength of the self-healed sensor versus tensile strain. j) Reflection wavelength changes of the repaired sensor during 100 finger bending/unbending cycles.

**ADVANCED
SCIENCE NEWS**
www.advancedsciencenews.com

**ADVANCED
FUNCTIONAL
MATERIALS**
www.afm-journal.de

sensor. The result shows that the reflection wavelength shifts from 637, 615, 595 to 576 nm at a bending angle of 0°, 30°, 60°, and 90°, respectively. At the same time, the motion amplitude can be read out directly through the change of structural color, indicating good visual interaction performance. Figure 5c shows the response of the sensor to the bending motion of the wrist. It is observed that the reflection wavelength switches 636 to 593 nm after bending. Obviously, the wavelength change of the finger motion is larger than that of the wrist, owing to relatively large bending amplitude. Similarly, the sensor also shows a stable response to the repeated motions of the elbow and knee (Figures 5d,e and Figures S12–S15, Supporting Information). These results reveal that the sensor has interactive sensing capability and stable visual response to the movement of human body. Conventional strain/stress sensors (such as resistance/capacitance sensors) are based on electrical signal transduction to sense external stimuli,[4c] which cannot be directly recognized by human eyes. In contrast, the photonic vitrimer sensor could sense external strains and stresses through color changes, which can be directly perceived by naked eyes, thus facilitating the direct intelligent interaction between users and devices.

In practical application, it is inevitable to encounter function loss due to the damage of sensing elements, such as scratch and cut. Interestingly, benefiting from the remarkable self-repairing performance of photonic vitrimer based on dynamic covalent bonds, the photonic vitrimer device still exhibits interactive sensing capability after self-repairing, when it suffers from scratch and fracture (Figure 5f). As shown in Figure 5g, the repaired sensor can also be used to detect the finger motion. It could be found that the color changes from red to green, and the reflection wavelength is shifted from 638 to 575 nm, which is comparable to the original performance (Figure S16, Supporting Information). To further verify the recovery of optical function, a stretching/releasing experiment of the repaired sensor was performed (Figure 5i). It is shown that there is a good correlation between the color and the strain. Particularly, the reflection wavelength and structural color keep stable even after 100 finger bending cycles (Figure 5j). Therefore, the repaired sensor demonstrates excellent optical function and durability, showing great promise in visualized interactive sensing.

3. Conclusions

In conclusion, we reported a self-healable photonic vitrimer elastomer based on the synergy of photonic crystal and vitrimer for the first time. The photonic crystal structure provides the photonic vitrimer with an optical function, while the vitrimer grants excellent mechanical properties. The resultant photonic vitrimer elastomer demonstrates outstanding performances including high toughness, bright structural color, mechanochromism, excellent creep resistance, and durability. Particularly, in situ healing of its optical function is achieved through the exchange of internal dynamic covalent bonds. Such features are otherwise difficult to achieve simultaneously for photonic crystal or neat vitrimer alone. Considering those merits, the photonic vitrimer is used as a robust interactive

sensor, allowing visualized sensing of human joints' motion behavior. The successful implementation of this work not only opens a door for optical functionalization of vitrimers, but also offers opportunities for their diverse applications in self-healable device, interactive sensing, wearable photonics, and textile graphic display (Figures S17–S19, Supporting Information).

4. Experimental Section

Materials: HTPB (M_n = 3000 g mol^{-1}) was purchased from Hefei Glen Technology Co. LTD. PTMG (Mn = 2000 g mol^{-1}) was purchased from Guangdong Wengjiang Chemical Reagent Co. LTD. Glycerin(GLY), IPDI, DBTDL, and triethoxyvinylsilane were purchased from Aladdin (Shanghai, China). Ammonium hydroxide and styrene were purchased from Tianjin Damao Chemical Reagent Factory. Sodium dodecyl sulfonate (SDS) and potassium persulfate were purchased from Tianjin Bodi Chemical Co. LTD.

Synthesis of PS and PS@SiO$_2$ Microspheres: PS and PS@SiO$_2$ microspheres suspensions were synthesized as previously reported in Liu, et al.[25] and Wu et al.[26]

Synthesis of Vitrimer Elastomers: First, HTPB, PTMG, and GLY were dried in a 120 °C vacuum oven for 4 h, then, HTPB, PTMG, GLY, and IPDI (Table S1, Supporting Information, shows the specific mass) were added into bottles at 60 °C. Thereafter, 1% DBTDL was sequentially added and vortexed. Then, the mixture was transferred to a Teflon mold and cured at 100 °C for 2 h. Finally, the cured sample was dried in a vacuum oven at 100 °C for 6 h.

Photonic Vitrimer Fabrication: The suspension of PS@SiO$_2$ microspheres was injected onto Teflon mold to assemble PS@SiO$_2$ opal photonic crystal template at 40 °C for 5 min. Then, the elastomer precursor composed of a mixture of HTPB, PTMG, GLY, IPDI, and DBTDL was infiltrated into the interstices of the above photonic crystal. After degassing for 30 min, the sample was cured at 100 °C for 2 h. Finally, the cured sample was dried in a vacuum oven at 100 °C for 6 h.

Fabric Printing: 1% PS@SiO$_2$ suspension in ethanol was sprayed onto the surface of a piece of black cotton cloth, forming the patterns of "DLUT" with the assistance of a mask. Vitrimer-II precursor was then infiltrated into the pattern area and cured at 70 °C for 4 h to form photonic vitrimer patterns. Controlling the size of PS@SiO$_2$ microsphere, a series of photonic patterns with different structural colors from red to blue were obtained.

Characterization: SEM images were obtained by a Nova NanoSEM 450. The normal-incidence optical reflection spectra and the changes in light reflection intensity at a specified wavelength were obtained using a PG2000-pro fiber optic spectrometer with a tungsten halogen light source (Shanghai Ideaoptics Corp., Ltd). Mechanical tensile test was carried out by a universe testing machine (PT-305, Dongguan Precise-Test Equipment Co., Ltd). FT-IR spectra were recorded on a 6700 spectrometer (ThermoFisher). XPS was recorded on a ESCALAB XI+ system (Thermo). ^{1}H-NMR spectra were recorded on a Bruker Avance NEO 600M NMR Spectroscopy. Thermogravimetric analysis (TGA) was conducted on a TA Q500 TGA tester (TA Instruments, USA). DMA was performed on a TA Q800 DMA tester (TA Instruments, USA). When applied to human motion monitoring, the sensor was fixed on various parts of the human body with tape. A spectrometer was used to monitor the light intensity at the specified wavelength in real-time. During the monitoring process, the vertical distance between the spectrometer probe and the moving part remained unchanged.

Supporting Information

Supporting Information is available from the Wiley Online Library or from the author.

[1] a) Y. Zou, V. Raveendran, J. Chen, *Nanotechnol. Energy* **2020**, *77*, 105303; b) Y. Yu, S. Peng, P. Blanloeuil, S. Wu, C. H. Wang, *ACS Appl. Mater. Interfaces* **2020**, *12*, 36578; c) C. Wang, K. Xia, H. Wang, X. Liang, Z. Yin, Y. Zhang, *Adv. Mater.* **2019**, *31*, 1801072.

[2] J. Deng, X. Kuang, R. Liu, W. Ding, A. C. Wang, Y. C. Lai, K. Dong, Z. Wen, Y. Wang, L. Wang, H. J. Qi, T. Zhang, Z. L. Wang, *Adv. Mater.* **2018**, *30*, 1705918.

[3] a) Y. Qi, L. Chu, W. Niu, B. Tang, S. Wu, W. Ma, S. Zhang, *Adv. Funct. Mater.* **2019**, *29*, 1903743; b) Y. Qi, W. Niu, S. Zhang, S. Wu, L. Chu, W. Ma, B. Tang, *Adv. Funct. Mater.* **2019**, *29*, 1906799.

[4] a) Q. Guo, B. Huang, C. Lu, T. Zhou, G. Su, L. Jia, X. Zhang, *Mater. Horiz.* **2019**, *6*, 996; b) Y. Wang, W. Niu, C. Y. Lo, Y. Zhao, X. He, G. Zhang, S. Wu, B. Ju, S. Zhang, *Adv. Funct. Mater.* **2020**, *30*, 2000356; c) H. Zhang, W. Niu, S. Zhang, *ACS Appl. Mater. Interfaces* **2018**, *10*, 32640; d) G. Kim, S. Cho, K. Chang, W. S. Kim, H. Kang, S. P. Ryu, J. Myoung, J. Park, C. Park, W. Shim, *Adv. Mater.* **2017**, *29*, 1606120.

[5] a) S. Yu, X. Cao, W. Niu, S. Wu, W. Ma, S. Zhang, *ACS Appl. Mater. Interfaces* **2019**, *11*, 22777; b) P. Wu, J. Wang, L. Jiang, *M. Horiz.* **2020**, *7*, 338.

[6] W. Guo, X. Wang, X. Lu, X. Li, Y. Li, J. Sun, *J. Mater. Chem. A* **2019**, *7*, 21927.

[7] a) Y. Fu, F. Xu, D. Weng, X. Li, Y. Li, J. Sun, *ACS Appl. Mater. Interfaces* **2019**, *11*, 37285; b) J. Xu, P. Chen, J. Wu, P. Hu, Y. Fu, W. Jiang, J. Fu, *Chem. Mater.* **2019**, *31*, 7951; c) B. Qin, S. Zhang, P. Sun, B. Tang, Z. Yin, X. Cao, Q. Chen, J. F. Xu, X. Zhang, *Adv. Mater.* **2020**, *32*, 2000096.

[8] a) C. H. Li, C. Wang, C. Keplinger, J. L. Zuo, L. Jin, Y. Sun, P. Zheng, Y. Cao, F. Lissel, C. Linder, X. Z. You, Z. Bao, *Nat. Chem.* **2016**, *8*, 618; b) L. Zhang, Z. Liu, X. Wu, Q. Guan, S. Chen, L. Sun, Y. Guo, S. Wang, J. Song, E. M. Jeffries, C. He, F. L. Qing, X. Bao, Z. You, *Adv. Mater.* **2019**, *31*, 1901402; c) S. Zhang, A. Hao, Z. Liu, J. G. Park, R. Liang, *Nano Lett.* **2019**, *19*, 3871; d) Q. Zhang, S. Niu, L. Wang, J. Lopez, S. Chen, Y. Cai, R. Du, Y. Liu, J. C. Lai, L. Liu, C. H. Li, X. Yan, C. Liu, J. B. Tok, X. Jia, Z. Bao, *Adv. Mater.* **2018**, *30*, 1801435.

[9] a) J. Sun, X. Pu, M. Liu, A. Yu, C. Du, J. Zhai, W. Hu, Z. L. Wang, *ACS Nano* **2018**, *12*, 6147; b) H. Zhang, Y. Wu, J. Yang, D. Wang, P. Yu, C. T. Lai, A. C. Shi, J. Wang, S. Cui, J. Xiang, N. Zhao, J. Xu, *Adv. Mater.* **2019**, *31*, 1904029; c) M. Chen, L. Zhou, Y. Wu, X. Zhao, Y. Zhang, *ACS Macro Lett.* **2019**, *8*, 255; d) T. Liu, C. Hao, L. Wang, Y. Li, W. Liu, J. Xin, J. Zhang, *Macromolecules* **2017**, *50*, 8588.

[10] D. Montarnal, M. Capelot, F. Tournilhac, L. Leibler, *Science* **2011**, *34*, 965.

[11] G. Zhao, Y. Zhou, J. Wang, Z. Wu, H. Wang, H. Chen, *Adv. Mater.* **2019**, *31*, 1900363.

[12] a) L. D. Bonifacio, B. V. Lotsch, D. P. Puzzo, F. Scotognella, G. A. Ozin, *Adv. Mater.* **2009**, *21*, 1641; b) E. Yablonovitch, *Phys. Rev. Lett.* **1987**, *58*, 2059; c) S. John, *Phys. Rev. Lett.* **1987**, *58*, 2486.

[13] a) S. Kinoshita, S. Yoshioka, K. Kawagoe, *Proc. R. Soc. London, Ser. B* **2002**, *269*, 1417; b) K. Creath, A. E. Luna, J. A. Shaw, D. C. Skigin, M. E. Inchaussandague, A. R. Alsina, *Nat. Light: Light Nat. III* **2010**, *7782*, 778205.

[14] G. H. Lee, T. M. Choi, B. Kim, S. H. Han, J. M. Lee, S. H. Kim, *ACS Nano* **2017**, *11*, 11350.

[15] X. Y. J. Zi, Y. Li, X. Hu, C. Xu, X. Wang, X. Liu, R. Fu, *Proc. Natl. Acad. Sci. U. S. A.* **2003**, *100*, 12576.

[16] a) S. Wu, H. Xia, J. Xu, X. Sun, X. Liu, *Adv. Mater.* **2018**, *30*, 1803362; b) S. Tadepalli, J. M. Slocik, M. K. Gupta, R. R. Naik, S. Singamaneni, *Chem. Rev.* **2017**, *117*, 12705; c) Y. Wang, Y. Yu, J. Guo, Z. Zhang, X. Zhang, Y. Zhao, *Adv. Funct. Mater.* **2020**, *30*, 2000151; d) P. Vukusic, J. R. Sambles, *Nature* **2003**, *424*, 852; e) J. Zhou, P. Han, M. Liu, H. Zhou, Y. Zhang, J. Jiang, P. Liu, Y. Wei, Y. Song, X. Yao, *Angew. Chem., Int. Ed.* **2017**, *56*, 10462; f) P. Han, X. He, Y. Zhang, H. Zhou, M. Liu, N. Wu, J. Jiang, Y. Wei, X. Yao, J. Zhou, Y. Song, *Adv. Opt. Mater.* **2019**, *7*, 1801749.

[17] H. Tan, Q. Lyu, Z. Xie, M. Li, K. Wang, K. Wang, B. Xiong, L. Zhang, J. Zhu, *Adv. Mater.* **2019**, *31*, 1805496.

[18] a) Y. Gong, Z. Chen, L. Yang, X. Ai, B. Yan, H. Wang, L. Qiu, Y. Tan, N. Witman, W. Wang, Y. Zhao, W. Fu, *ACS Nano* **2020**, *14*, 8232; b) L. Li, Z. Chen, C. Shao, L. Sun, L. Sun, Y. Zhao, *Adv. Funct. Mater.* **2019**, *30*, 1906353.

[19] a) D. Fan, G. Wang, A. Ma, W. Wang, H. Chen, L. Bai, H. Yang, D. Wei, L. Yang, *ACS Appl. Mater. Interfaces* **2019**, *11*, 38126; b) S. Xiong, J. Fan, Y. Wang, J. Zhu, J. Yua, Z. Hu, *J. Mater. Chem. A* **2017**, *5*, 18242; c) A. S. Subramanian, J. N. Tey, L. Zhang, B. H. Ng, S. Roy, J. Wei, X. M. Hu, *Polymer* **2016**, *82*, 285.

[20] H. Liu, *Handbook of Polyurethane Elastomer*, Chemical Industry Press, Beijing **2012**.

[21] a) Z. Liu, L. Zhang, Q. Guan, Y. Guo, J. Lou, D. Lei, S. Wang, S. Chen, L. Sun, H. Xuan, E. M. Jeffries, C. He, P. L. Qing, Z. You, *Adv. Funct. Mater.* **2019**, *29*, 1901058; b) S. M. Kim, H. Jeon, S. H. Shin, S. A. Park, J. Jegal, S. Y. Hwang, D. X. Oh, J. Park, *Adv. Mater.* **2018**, *30*, 1705145.

[22] A. J. Kinneging, *J. Chem. Educ.* **1993**, *70*, 451.

[23] a) M. Li, H. Tan, L. Jia, R. Zhong, B. Peng, J. Zhou, J. Xu, B. Xiong, L. Zhang, J. Zhu, *Adv. Funct. Mater.* **2020**, *30*, 2000008; b) M. Li, B. Zhou, Q. Lyu, L. Jia, H. Tan, Z. Xie, B. Xiong, Z. Xue, L. Zhang, J. Zhu, *Mater. Chem. Front.* **2019**, *3*, 2707; c) L. Jia, M. Li, L. Jiang, H. Gao, H. Tan, B. Peng, J. Xu, L. Zhang, J. Zhu, *J. Mater. Chem. C* **2020**, *8*, 9286; d) J. Chen, L. Xu, M. Yang, X. Chen, X. Chen, W. Hong, *Chem. Mater.* **2019**, *31*, 8918; e) G. W. T. Cai, S. Thompson, M. Marquez, Z. Hu, *Macromolecules* **2008**, *41*, 9508.

[24] Y. Qiao, Y. Li, W. Li, J. Bao, Y. Zheng, L. Feng, Y. Ma, K. Yang, A. Wu, H. Bai, Y. Yang, *New J. Chem.* **2020**, *44*, 1107.

[25] F. Liu, B. Shan, S. Zhang, B. Tang, *Langmuir* **2018**, *34*, 3918.

[26] J. Wu, W. Niu, S. Zhang, S. Wu, W. Ma, B. Tang, *New J. Chem.* **2019**, *43*, 11517.